scientific reports

Check for updates

OPEN

Ectomycorrhizal fungal community varies across broadleaf species and developmental stages

Dong-Xue Zhao[1,2,4], Zhen Bai[1,4], Yi-Wei Yuan[3], Si-Ao Li[1,2], Yu-Lian Wei[1] & Hai-Sheng Yuan[1]✉

Ectomycorrhizal fungi (EMF) play pivotal roles in determining temperate forest ecosystem processes. We tracked root EMF community succession across saplings, juveniles, and adults of three temperate broadleaf trees (*Acer mono*, *Betula platyphylla*, and *Quercus mongolica*) in Northeast China. Adult stages showed higher alpha diversity but lower community dissimilarity compared to earlier stages. In particular, the EMF alpha diversity of *Quercus mongolica* marginally increased along with host developmental stages and ranked as sapling < juvenile < adult. Unlike those of *Acer mono* and *Quercus mongolica*, the EMF community composition of *Betula platyphylla* showed greater variation between the sapling and juvenile stages than between the sapling and adult stages. Cooccurrence networks revealed increasing interconnectivity with host maturity, dominated by positive correlations (> 99%). LEfSe was employed to identify stage- and/or host-specific EMF indicators. This study highlighted the assembly of EMF community during the development of broadleaf trees in temperate forests, thereby advancing understanding of the succession and coevolution of symbiotic relationships.

Keywords Broadleaf trees, Community assembly, Developmental stage, Ectomycorrhizal fungi (EMF), Root tips

Ectomycorrhizal fungi (EMF) form mutualistic relationships with plant roots, where their extramatrical mycelia extend many centimeters into soil, facilitating root nutrient (e.g., nitrogen) uptake and, in turn, receiving photosynthesized carbon from host plant[1,2]. This symbiosis is crucial for the survival, health, and growth of temperate forests[3,4]. For example, EMF hyphae enable plants to access a larger soil bank[5], secrete hydrolytic exoenzymes to mobilize nutrients from soil mineral–organic matter[6], and trigger plant defense mechanisms against pathogens and abiotic stressors[7]. Broadleaf trees in temperate forests, particularly those of the Betulaceae, Fagaceae and Sapindaceae families, rely heavily on EMF symbiosis for establishment and growth[8]. Investigating the assembly of the root EMF communities during host development is essential for understanding the survival strategies of these obligately ectomycorrhizal trees in temperate ecosystems[8].

Previous studies document that EMF diversity increases as hosts mature. For instance, EMF richness of *Quercus liaotungensis* notably increases across sapling (1–3 years), juvenile (20–30 years) and mature stage (50–70 years)[9]. Similarly, the Shannon index of *Fagus* sylvatica EMF rises as hosts mature from early (~ 20 years) to later stages (~ 100 years)[10]. These shifts are attributed to the expansion of well-established root systems in adult trees, which allows for greater soil exploration and facilitates the recruitment of new fungal species via ectomycorrhizal networks (EMNs) shared by neighboring trees[8]. Albeit typically increasing with host maturity, EMF richness and evenness may decrease at very late host stages due to the competitive pressures of conspecific neighbors, which can elevate mortality rates via species-specific pathogens[11–14]. In contrast, a study on *Betula papyrifera* suggests minimal changes in EMF diversity between the host stages of 5 and 65 years, probably because paper birch regenerates through stump sprouts and thereby maintains the host-specific EMF[15]. In addition, *Corylus avellana* exhibits little variation in EMF community composition between the ages of 50–100 years and 100–200 years, with younger (< 50 years) stages differing more significantly[16]. Furthermore, the EMF community compositions of young (20–30 years) and mature (50–70 years) *Quercus liaotungensis* are more similar to each other than to saplings (1–3 years)[9]. These suggest that adult host trees serve as major key repositories of forest biomass and pivotal hubs in EMNs, facilitating local coexistence of EMF[17,18]. Despite extensive research on the EMF of broadleaf trees, few studies have examined the effects of host development across multiple coexisting tree species[19–22].

[1]CAS Key Laboratory of Forest Ecology and Silviculture, Institute of Applied Ecology, Chinese Academy of Sciences, Shenyang 110164, P. R. China. [2]University of the Chinese Academy of Sciences, Beijing 100049, P. R. China. [3]College of Life Sciences, Shanxi Agricultural University, Taigu, Shanxi 030801, P. R. China. [4]Dong-Xue Zhao and Zhen Bai contributed equally to this work. ✉email: hsyuan@iae.ac.cn

The zonal top broadleaf Korean pine mixed forests in Changbai Mountain are renowned for their high biodiversity and complex stand structure[23]. For instance, the second poplar–birch forests, which developed following disturbances in the original broadleaf Korean pine forests, mainly comprise of *Betula platyphylla* and *Populus davidiana*. These forests serve as vital repositories of various EMF symbionts and are relatively short-lived, typically declining after 50–60 years[24]. This study aims to investigate the succession patterns of root EMF communities across the sapling, juvenile, and adult stages of three typical broadleaf trees—*Acer mono*(Sapindaceae), *Betula platyphylla*(Betulaceae) and *Quercus mongolica*(Fagaceae). By utilizing Illumina MiSeq sequencing, we examine root EMF communities and identify specific EMF taxa associated with each host species and developmental stage. The correlations among the root EMF ASVs across different developmental stages were statistically analyzed.

Results

Database and major EMF taxa

After quality control and denoising, we obtained 1,153,982 high-quality concatinated nonchimeric reads from 3,875,730 raw paired-end reads across 77 root samples. These sequences were mapped to 5,726 amplicon sequence variants (ASVs), of which 1,108 ASVs (579,294 sequences) were identified as EMF species (Supplementary Table S2). These EMF ASVs spanned major phyla of Basidiomycota and Ascomycota, families such as Thelephoraceae, Russulaceae, Sebacinaceae, and Inocybaceae (Supplementary Fig. S2). The dominant EMF genera (>1%) were *Tomentella*, *Russula*, *Inocybe*, *Sebacina*, *Tuber*, *Cortinarius*, *Amphinema*, *Humaria*, *Cenococcum*, *Piloderma*, *Trichophaea*, *Lactarius*, *Leccinum*, *Phaeohelotium*, and *Thelephora*(Supplementary Fig. S3).

Alpha diversity of the EMF

We compared the alpha diversity (such as Observed number of ASVs, Shannon, Simpson, Chao1, ACE, and Pielou indices) differences of root EMF by Kruskal–Wallis test to discern the patterns of fungal richness as influenced by the maturation of hosts (Supplementary Table S3, Fig. 1). Furthermore, the EMF alpha diversity indices (Observed number of ASVs, Chao1, ACE) were significantly influenced by the tree species at particular developmental stages ($P<0.001$, Supplementary Table S3). For example, from sapling to juvenile stage, EMF diversity remained relatively stable in *Acer mono*($P>0.05$), marginally decreased in *Betula platyphylla*($0.05<P<0.1$), whereas marginally increased in *Quercus mongolica*($0.05<P<0.1$). Moreover, at the sapling stage, EMF diversity was significantly higher in *Betula platyphylla* than in *Acer mono* and *Quercus mongolica*($P<0.05$). At the juvenile stage, EMF diversity ranked as *Acer mono*<*Betula platyphylla*<*Quercus mongolica*($P<0.05$). Unlike those at the early stages, the EMF diversity in the adult hosts did not significantly vary across tree species ($P>0.05$, Supplementary Fig. S4). The above results implicate that as hosts mature, the

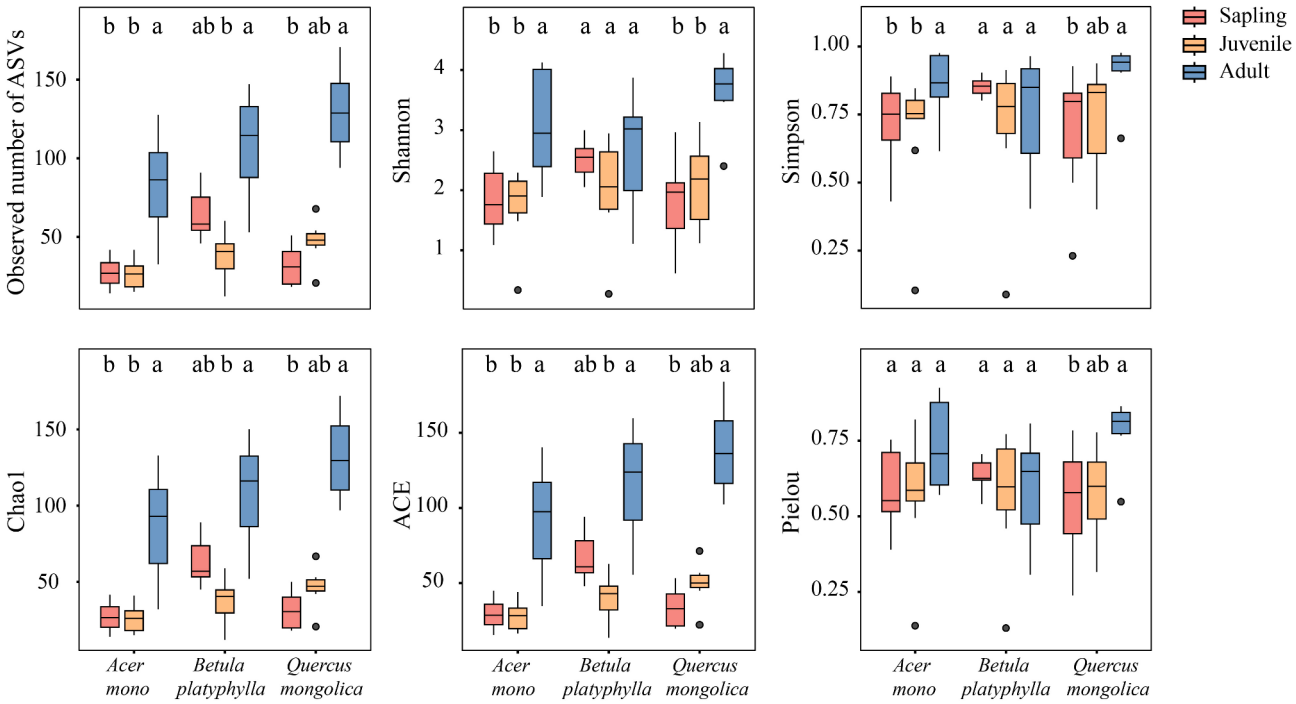

Fig. 1. Alpha diversity indices of the ectomycorrhizal fungi (EMF) at the different developmental stages of the three broadleaf trees. The differences at the various developmental stages were examined via one-way analysis of variance (ANOVA) or the Kruskal–Wallis test. The Kruskal–Wallis test was applied for alpha diversity indices that failed to meet the homogeneity of variance (Levene's test) and normality requirements (Kolmogorov–Smirnov test). The different letters above the columns indicate significant differences between stages ($P<0.05$).

EMF diversity increases and transitions from early-stage heterogeneity to late-stage convergence among the different host species.

Beta diversity of the EMF

Nonmetric multidimensional scaling (NMDS) and Permutational multivariate analysis of variance (PERMANOVA) demonstrated significant compositional shifts across stages ($P < 0.001$, Fig. 2a), with adult communities showing lower dissimilarity among tree individuals ($P < 0.05$, Fig. 2b; Supplementary Fig. S5). Particularly, unlike *Acer mono* and *Quercus mongolica*, the EMF communities in *Betula platyphylla* were not significantly different between the sapling and adult stages ($P > 0.05$, Fig. 2). Our findings indicate that the variance in the root EMF communities among the different hosts decrease markedly with host maturity, revealing a trend toward age-related convergence in the root EMF community composition.

Cooccurrence network analysis of the EMF

To explore the interaction patterns within EMF communities, we constructed a meta-community cooccurrence network based on Spearman's correlation ($P < 0.05$) and examined how these networks varied with host maturity and tree species. We identified stage-specific EMF taxa and categorized them into four clusters: sapling-, juvenile-, and adult-enriched ASVs, along with a set of common ASVs (Fig. 3). Cooccurrence network demonstrated high degrees of positive correlations among EMF taxa (positive correlations exceeding 99%, Supplementary Table S4) in all three tree species: 6,290 correlations (edges) among 501 ASVs (nodes) for *Acer mono*, 7,471 edges and 631 nodes for *Betula platyphylla*, and 11,983 edges and 540 nodes for *Quercus mongolica*. The modularity values were greater than 0.4 (Supplementary Table S4), indicating that the networks exhibited distinct modular structures. The node-level topological features (degree, closeness centrality, and eigenvector centrality) were significantly greater at the adult stage compared to earlier stages ($P < 0.05$, Supplementary Fig. S6). Furthermore, the adult-stage subnetworks encompassed more nodes and edges, higher average degree and graph density, but lower average path length and diameter, relative to its earlier stages (Supplementary Table S4). These findings demonstrate that the EMF communities are more aggregated and cohesive with host maturity, occupying a central position in cooccurrence networks.

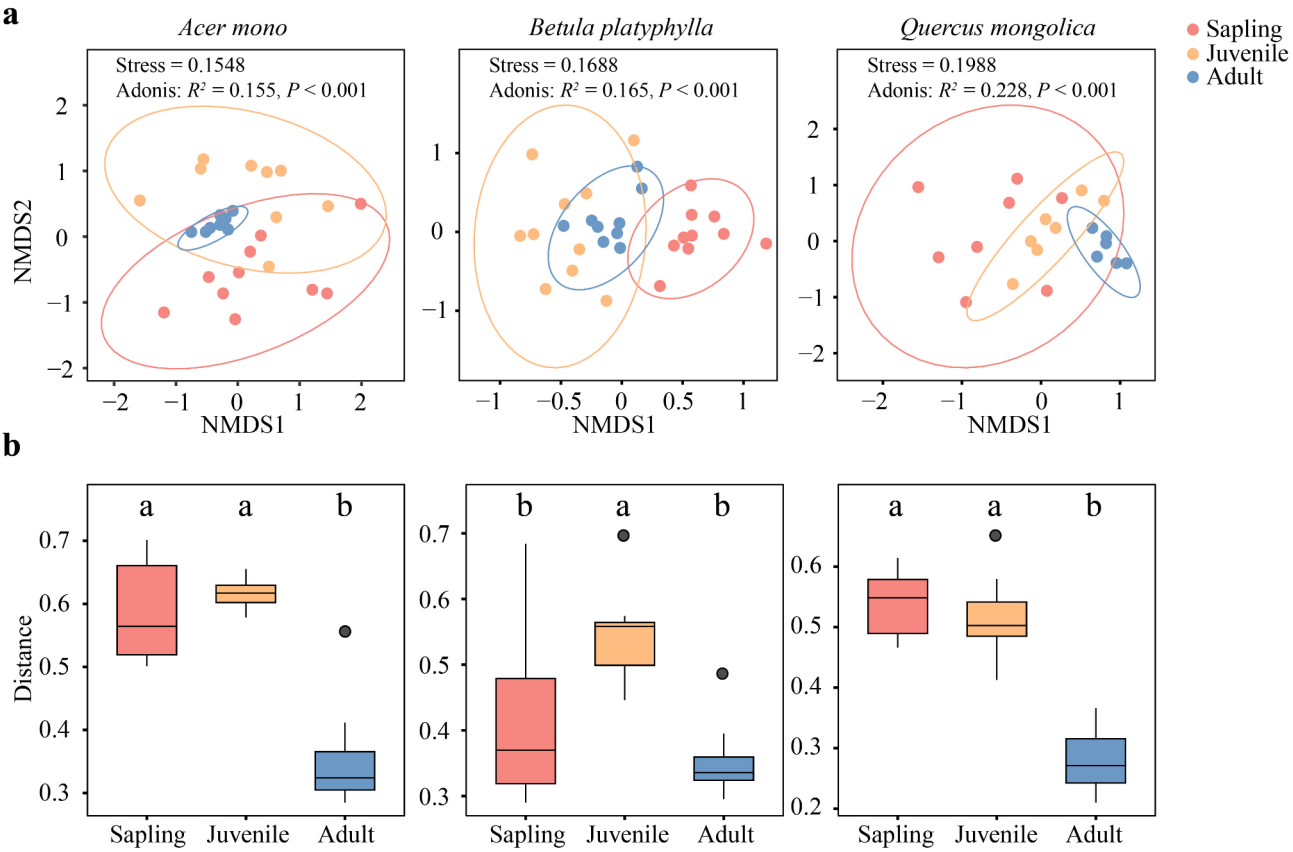

Fig. 2. Community composition of the ectomycorrhizal fungi (EMF) at the different developmental stages of the three broadleaf trees. (**a**) Nonmetric multidimensional scaling (NMDS) and Permutational multivariate analysis of variance (PERMANOVA). The ellipses delimit 95% confidence intervals around centroids for each developmental stage. (**b**) The Bray–Curtis dissimilarity distances among tree individuals of different developmental stage. The different letters above the columns indicate significant differences between developmental stages (Kruskal–Wallis test, $P < 0.05$).

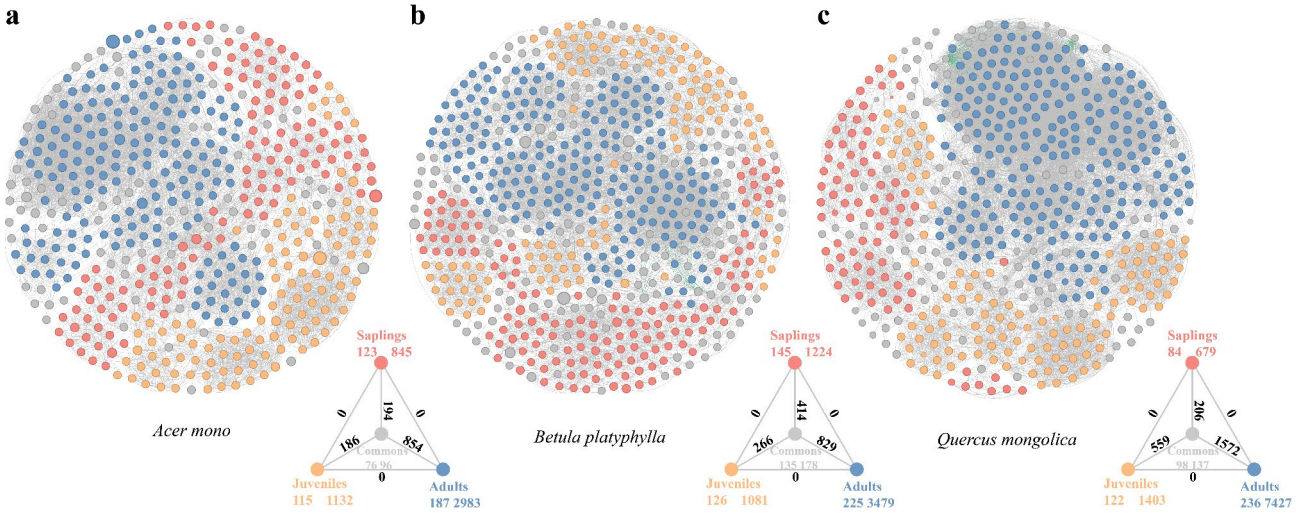

Fig. 3. Cooccurrence networks of the stage-enriched ASVs of ectomycorrhizal fungi (EMF) for *Acer mono*(**a**), *Betula platyphylla*(**b**), and *Quercus mongolica*(**c**). Each node represents an EMF ASV, and the node size is proportional to the relative abundance of an ASV. The edges represent a strong correlation (Spearman's $r > 0.6$) and significance (corrected false discovery rate $P < 0.01$). The stage-enriched ASVs in the networks are distinguished by color-coded points, namely, those at the sapling stage are marked in light red, those at the juvenile stage are marked in light yellow, and those at the adult stage are marked in light blue. The ASVs that exist across tree ages are considered common and are marked in gray. Node–edge interaction information is provided in the lower right corner of each network. The numbers of nodes and edges are shown in different colors according to the corresponding categories. The black numbers above the line indicate external associations between two groups. The gray edges denote positive relationships, and the green edges denote negative relationships among the ASVs in the networks.

Stage-associated indicators of specific host species

To identify key ASVs driving EMF community assembly, we conducted linear discriminant analysis (LDA) effect size (LEfSe) to detect EMF indicators of specific host species and stage. As for *Acer mono*, the adult stage was predominated by 20 EMF species primarily belonging to Atheliales and Pilodermataceae; the earlier stages were enriched in Pyronemataceae, Boletales and *Russula vinosobrunneola*. As for *Quercus mongolica*, the adult stage were dominated by 19 EMF species predominantly belonging to Atheliales, Pilodermataceae, *Thelephora* sp., and *Cenococcum* sp.; the sapling and juvenile stages were closely associated with *Thelophora* sp. and *Elaphomyces papillatus*. *Betula platyphylla* exhibited 11 EMF species enriched at the sapling stage and 7 EMF species at the later stages. Moreover, certain EMF indicators were common across tree species at specific development stages: the sapling stage was specifically abundant with Agaricales, Inocybaceae, Tylosporaceae and *Amphinema*; the juvenile stage with *Russula* and Pyronemataceae; and the adult stage with *Russula font-queri*, Cortinariaceae and Suillaceae (Fig. 4, Supplementary Fig. S7).

Discussion

To explore the dynamics of EMF communities in coexistent broadleaf trees at a regional scale, we analyzed 77 root tips from a chronosequence encompassing sapling, juvenile, and adult stages in temperate forests of Northeast China. EMF alpha diversity was significantly higher in adult trees than their younger counterparts. Furthermore, EMF community composition diverged to a greater extent during early host development, with mature trees hosting more converged EMF community composition. Cooccurrence network analysis confirmed that, as trees mature, EMF taxa became increasing integrated, displaying higher centrality, connectivity, and modularity. This suggests that mature trees foster more robust mutualistic networks, enhancing symbiotic interactions.

Mature broadleaf trees tended to host EMF communities with lower alpha diversity but higher structural dissimilarity compared to saplings and juveniles, consistent with previous studies[15,19]. This can be attributed to the limited contact with EMF spores in undeveloped root systems of early-stage hosts[25]. These young pioneers also face higher mortality rates due to environmental stressors such as nutrient depletion, moisture stress, herbivore damage, and wind disturbance[26]. However, mature trees benefit from fully extended root systems that connect them to a broader range of EMF species, leading to more stable nutrient and water acquisition and increased EMF diversity[27–29]. These long-term obligate symbioses may streamline EMF partners and optimize nutrient-use-efficiency, facilitating adaptations to similar biotic and abiotic stressors over the host's life span[30]. Across premature host stages, the stochastic EMF recruitment[25], compounded by environmental stressors, disrupt the continuity of the mycorrhizal networks, increasing the divergence of the EMF communities[26]. While we did not directly examine whether the EMF community of younger trees is nested within that of mature individuals, this remains a plausible hypothesis for future investigation.

Network analysis demonstrated increased EMF integration in mature hosts, with higher modularity and centrality suggesting stabilized and interconnected mutualistic networks. This pattern aligns with prior findings

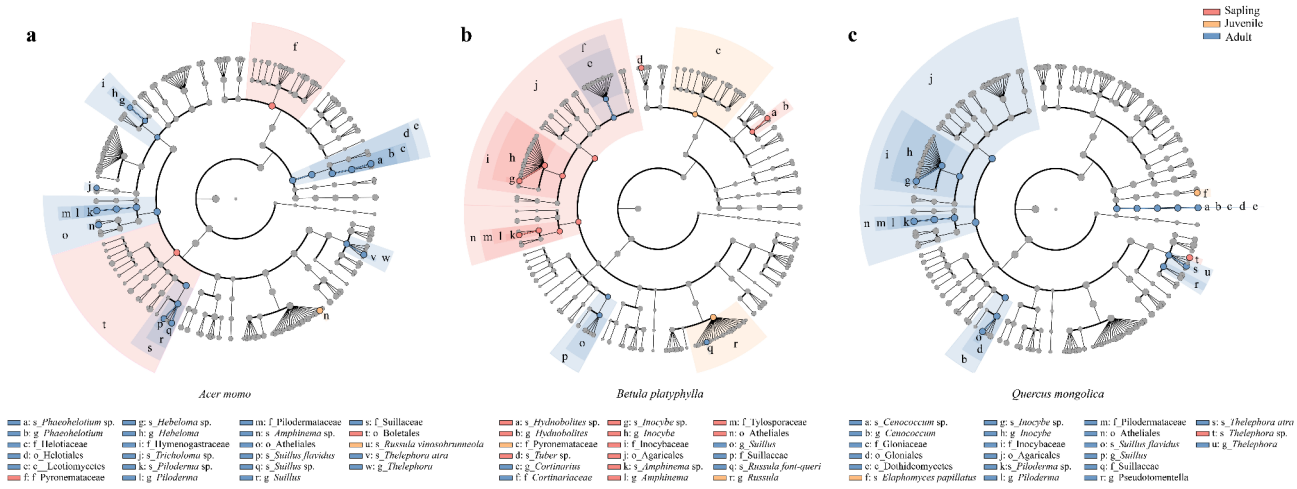

Fig. 4. Cladogram showing the phylogenetic distribution of the ectomycorrhizal fungi (EMF) of *Acer mono*(**a**), *Betula platyphylla*(**b**), and *Quercus mongolica*(**c**). The threshold of LDA score was 4.0. The gray circles denote taxa with no significant differences, and other colored circles denote significant differences in abundance at the corresponding stages. The rings of the cladogram show the kingdom, phylum, class, order, family, genus and species from inside to outside.

on the stability of adult-hosted EMF communities[29,31,32] as long-lived trees selectively recruit EMF to synchronize growth and facilitate community convergence. Even though stage-specific EMF did not always directly interact, they were consistently linked to common EMF species, especially in adult hosts. This suggests that the evolution of stage-specific EMF communities heavily rely on common species that mediate the development of mutualistic networks during host maturation[33]. We found that positive associations among EMF species predominated (over 99%), which likely stems from niche overlap, ecological compatibility, and resource exchange. This promotes plant-soil feedbacks, supports plant maturation, and contributes to forest succession[34]. The minimal negative correlations between stage-specific and common EMF species suggest low competition, facilitating the equilibrium and coexistence of EMF species[35].

Several EMF taxa demonstrated broad host spectra across multiple developmental stages. For instance, *Suillus* is known as an obligate symbiont of Pinaceae and can significantly alters the morphology and hormone content in host seedlings[36], and it also benefits the growth of *Quercus*[37]. The mixed forest composition at the current sites supports the likelihood of multihost colonization, highlighting a trend towards symbiotic promiscuity rather than specificity. Furthermore, the host preference of *Suillus* underscores the evolutionary constraints of EMF species[38], as its persistence in mature hosts reflects legacy effects of past host community dynamics[39]. Moreover, the adult-stage indicator *Plioderma*, found in *Acer mono* and *Quercus mongolica*, is adapted to low nitrogen availability and typically associated with late-stage hosts[40–42]. This indicates that trees at very late developmental stages acquire resources via specific EMF species, thereby supporting their persistence across different succession stages[43]. EMF species adopt different life strategies at various stages of host development. For example, Pyronemataceae, adapted to nutrient-poor environments[44], are suitable partners for *Acer mono* saplings that thrive in highly heterogonous niches[45]. Additionally, *Inocybe* and *Amphinema*, preferring nutrient-rich and disturbed environments, aid the establishment of *Betula platyphylla* in post-disturbance sites[46]. In contrast, *Russula* prefers mature forests, probably due to challenges with spore dispersal and germination at early developmental stages of hosts[15,47]. In addition, we also observed that *Acer mono* adults were predominated by *Phaehelotium* and *Hebeloma*, and *Quercus mongolica* adults by *Cenococcum* and *Thelephora*. All these families are optimized for short-distance exploration[48], maximizing hydrophilic hyphal extension to efficiently absorb nutrients and enabling energy-conserving late-stage growth.

Conclusion

In summary, we revealed root EMF dynamics and succession across the various development stages of broadleaf trees in Changbai Mountain. The transition from early-stage heterogeneity to late-stage homogeneity illustrates adaptive strategies of symbiontic relationships as host trees mature. This suggests a natural selection process driving the convergence of symbiotic networks, which is crucial for the survival and success of heterospecifics in temperate forests. This adaptive mechanism helps select specific EMF partners as keystone taxa to the hosts at each stage. The EMF–host relationship is not strictly species-specific but exhibits overlap as hosts mature. This highlights the succession of EMF and contributes to understanding how these interactions evolve within forest ecosystems. These insights lay a framework for further investigations on the mechanisms underlying EMF dynamics and implications for the management and protection of forests.

Materials and methods

Experimental site

The study was conducted in the National Nature Reserve on the northern slope of Changbai Mountain (41°43′ N to 42°26′ N, 127°42′ E to 128°17′ E), northeastern China. This region expriences a temperate continental monsoon climate, with an annual average temperature of 2.8 °C (January average: -13.7 °C; July average: 19.6 °C) and annual precipitation of approximately 700 mm, mainly occurring in June and August[49]. The reserve, established in 1960, spans 200,000 ha and ranges in elevation from 740 m to 2691 m. Five vegetation zones are present: aspen-white birch (*Populus davidiana* and *Betula platyphylla*) forests, broadleaf Korean pine (*Pinus koraiensis*) mixed forests, spruce-fir (*Picea jezoensis* and *Abies nephrolepis*) forests, subalpine birch (*Betula ermanii*) forests, and alpine tundra[50], and the broadleaf Korean pine mixed forests, predominantly composed of *Pinus koraiensis*, *Tilia amurensis*, *Quercus mongolica*, *Fraxinus mandshurica*, and *Acer mono*[50]. The three tree species investigated were: *Acer mono*(Sapindaceae), at an elevation of 850 ± 50 m; *Betula platyphylla*(Betulaceae), at an elevation of 900 ± 50 m; and *Quercus mongolica*(Fagaceae), at an elevation of 950 ± 50 m. These species grow in broadleaf Korean pine mixed forests, secondary poplar–birch forests, and secondary coniferous-broadleaved mixed forests, respectively.

Tree classification and sampling

To examine how tree ontogeny influences EMF communities, trees were classified into three developmental stages based on diameter at breast height (DBH) as a proxy for tree age[15,51]: saplings (DBH < 5 cm), juveniles (DBH 5–20 cm), and adults (DBH > 20 cm) (Supplementary Table S1). Sampling was conducted in July 2019 at three distinct sites, with each site representing each host identity with all three developmental stages (Supplementary Fig. S1)[52,53]. At each site, 10 individual trees per developmental stage were randomly selected, with at least 20 m between individuals. Fine roots were excavated in three directions along the taproots, and the roots from all directions were combined into a single sample for each individual tree. All the saplings were removed from the soil because of the limited number of root systems. A total of 90 root samples (three tree species × three stages × ten replicates) were collected. All saplings were removed due to limited root systems. Samples were transported on ice to the laboratory and stored at -20 °C before processing.

DNA extraction

Before molecular analysis, we washed away any residual soil clinging to the fine roots under running tap water and cut them into small root segments. Approximately 400 root tips were randomly obtained from each sample under a stereomicroscope and ground into powder with the aid of liquid nitrogen. We selected all the root tips of the sampled saplings (< 200) as a result of their undeveloped root systems. Total root genomic DNA was extracted from 0.5 g of powder via an FH Plant DNA Kit following the manufacturer's instructions (Beijing Demeter Biotech Co., Ltd., Beijing, China). The quality and concentration of DNA were measured via the optical density (OD) at 260/280 nm on a Thermo Scientific NanoDrop 2000 spectrophotometer, and values ranging from 1.8 to 2.0 were selected for downstream polymerase chain reaction (PCR) amplification.

PCR amplification and illumina sequencing

The internal transcribed spacer 2 (ITS2) was amplified from the extracted DNA via the primers ITS3tagmix (5′-CATCGATGAAGAACGCAG-3′)[54] and ITS4NGS (5′-TCCTSCGCTTATTGATATGC-3′)[54]. PCRs were performed in 25-μL solutions containing 2.5 μL of DNA template, 12.5 μL of KAPA HiFi HotStart ReadyMix (Thermo Scientific, Waltham, MA, USA) and 1 μM of each primer. The PCR program began with initial denaturation at 95 °C for 3 min, followed by 25 cycles of 95 °C for 30 s, 55 °C for 30 s, and 72 °C for 30 s, and a final extension at 72 °C for 5 min. Under the same reaction conditions, we replaced the extracted DNA with nuclease-free water as a negative control to ensure successful amplification.

Nextera XT Index primers (Illumina, San Diego, CA, USA) with N7 (S5) were employed as the forward (reverse) reads for the second round of PCR amplification. The 50-μL reaction mixtures comprised 5 μL of DNA, 10 μL of PCR-grade water, 25 μL of KAPA HiFi HotStart ReadyMix, 5 μL of N7xx primers and 5 μL of S5xx primers. The reaction was performed at 95 °C for 3 min, followed by 8 cycles of 95 °C for 30 s, 55 °C for 30 s, and 72 °C for 30 s, and a final extension at 72 °C for 5 min. The PCR products obtained were cleaned with AMPure magnetic beads (Beckman Coulter Life Sciences, Indianapolis, IN, USA). The purified PCR products were pooled at equimolar concentrations for amplicon library preparation and sequencing, which were completed on an Illumina MiSeq platform (Illumina, San Diego, CA, USA) at the Testing and Analysis Center, Institute of Applied Ecology, Chinese Academy of Sciences.

Sequence processing

Raw paired-end reads were analyzed via QIIME2 2020.11[55]. The DADA2[56] was used for quality filtering, denoising, chimera removal, and ASVs generation. Low-quality sequences were trimmed fro the 3' ends, with forward and reverse sequences cut at position 280 and 220, respectively. Taxonomic assignment of fungal sequences was performed against the UNITE + INSDC fungal ITS database (version 8.3)[57]. EMF taxa were identified according to genuslevel functional annotations from the Fungaltraits database[48]. Due to uneven sequence depths between samples, rarefaction was used to normalize each ample to a minimum depth of 24,576 sequences, a threshold chosen to ensure statistical power and representativity s[12,58]. The final dataset consisted of 77 samples, after excluding low-quality samples. Raw sequencing data were deposited into the NCBI Sequence Read Archive (SRA) database (BioProject ID: PRJNA1051329).

Statistical analysis

Taxonomic assignments were visualized via a cladogram through the head_tree function in the metacoder package[59]. The effects of developmental stage and tree species on the EMF community were tested using generalized linear mixed models implemented via the glmer function in the lme4 package (v1.1-35)[60]. Alpha diversity indices (Chao1, ACE, Shannon, Simpson, and Pielou) were estimated with estimateR and diversity functions from the vegan package (v2.6-4). NMDS with Bray–Curtis dissimilarity distances (metaMDS function) visualized community composition similarity. PERMANOVA (adonis2 function with 999 permutations) tested stage-driven compositional differences. The EMF diversity indices and community compositional differences among various developmental stages were examined as follows. Normality was evaluated via Shapiro-Wilk tests (shapiro_test in rstatix v0.7.2); Homoscedasticity via Levene's test (levene_test). Where assumptions were violated (e.g., Simpson index: $W = 0.872$, $p = 0.012$), non-parametric Kruskal-Wallis tests (kruskal_test) with Dunn's post-hoc comparisons (dunn_test) replaced one-way ANOVA. All p-values were adjusted via Benjamini-Hochberg false discovery rate control[61].

Cooccurrence networks of the EMF communities were constructed for each tree species with the igraph package[62]. The nodes represented the EMF ASVs, the edges represented correlations between EMF ASVs. Only robust correlations with Spearman's correlation coefficients (r) > 0.6 or < -0.6 and Benjamini – Hochberg false discovery rate (FDR)-adjusted P values < 0.01 were retained to establish networks[63]. To explore stage-discriminatory patterns, ASVs unique to a given stage were defined as stage-enriched ASVs. Pairwise paired t-test were applied to compare the relative abundance of each ASV among the different developmental stages, with no-significant differences indicating common ASVs. To reflect network aggregation and cohesion, we calculated network-level metrics, including average degree, clustering coefficient, and graph density[64]. The average path length was derived to measure network connectivity and dispersion[65]. Furthermore, the diameter was used to assess the network size and scale[66]. At the node level, we calculated degree, betweenness, closeness, and eigenvector centrality. Degree denotes the number of connections per node; betweenness centrality measures a node's role as a bridge; closeness centrality represents the average shortest path between nodes; and the eigenvector centrality indicates the influence of a node based on its neighbors' centrality[67]. Cooccurrence networks were visualized with the interactive platform Gephi 9.0[68].

To describe and verify distinct species at specific developmental stages, LEfSe analysis was adopted to discover stage-associated EMF indicators via classification comparison, biological consistency testing, and effect size estimation[69]. First, we used the Kruskal–Wallis test to identify EMF taxa with significant abundance differences across different stages. The Wilcoxon rank sum test method was subsequently employed to determine whether these significantly different taxa converged to the same classification within each stage. Finally, the LDA was applied, with an LDA score threshold of 4 and a significant threshold of $P < 0.05$ to identify stage-specific indicators. LEfSe analysis was conducted using the Galaxy platform[70].

Data availability

The raw sequencing reads obtained from the Illumina MiSeq platform were deposited in the NCBI Sequence Read Archive under accession no. PRJNA1051329 and are publicly available as of the date of publication. Please contact the corresponding author for further information if necessary.

Received: 28 November 2024; Accepted: 20 February 2025
Published online: 26 February 2025

References

1. Cairney, J. W. G. Extramatrical mycelia of ectomycorrhizal fungi as moderators of carbon dynamics in forest soil. *Soil Biol. Biochem.* **47**, 198–208 (2012).
2. Clasen, B. et al. Characterization of ectomycorrhizal species through molecular biology tools and morphotyping. *Scientia Agricola*. **75**(3), 246–254 (2018).
3. Mitra, D. et al. Impacts of arbuscular mycorrhizal fungi on rice growth, development, and stress management with a particular emphasis on strigolactone effects on root development. *Commun. Soil Sci. Plant Anal.* **52**(14), 1591–1621 (2021).
4. Bosso, L. et al. Plant pathogens but not antagonists change in soil fungal communities across a land abandonment gradient in a Mediterranean landscape. *Acta Oecol.* **78**, 1–6 (2017).
5. Lundberg-Felten, J., Martin, F. & Legue, V. Signalling in ectomycorrhizal symbiosis. *Signal. Communication Plants*. **11**, 123–142 (2011).
6. Landeweert, R. et al. Linking plants to rocks: ectomycorrhizal fungi mobilize nutrients from minerals. *Trends Ecol. Evol.* **16**(5), 248–254 (2001).
7. Wang, Y. H., Dai, Y., Kong, W. L., Zhu, M. L. & Wu, X. Q. Improvement of sphaeropsis shoot blight disease resistance by applying the ectomycorrhizal fungus *Hymenochaete* sp. Rl and mycorrhizal helper bacterium *Bacillus pumilus* HR10 to *Pinus thunbergii*. *Phytopathology* **112**(6), 1226–1234 (2022).
8. Ishida, T. A., Nara, K. & Hogetsu, T. Host effects on ectomycorrhizal fungal communities: insight from eight host species in mixed conifer-broadleaf forests. *New Phytol.* **174**(2), 430–440 (2007).
9. Zhang, J. et al. Ectomycorrhizal fungal communities of *Quercus liaotungensis* along different successional stands on the Loess Plateau, China. *J. For. Res.* **19**(4), 395–403 (2014).
10. Rosinger, C., Sandén, H., Matthews, B., Mayer, M. & Godbold, D. L. Patterns in ectomycorrhizal diversity, community composition, and exploration types in European beech, pine, and spruce forests. *Forests* **9**(8), 445 (2018).
11. Odriozola et al. Stand age affects fungal community composition in a central European temperate forest. *Fungal Ecol.* **48**, 100985 (2020).
12. Birch, J. D., Lutz, J. A., Turner, B. L. & Karst, J. Divergent, age-associated fungal communities of *Pinus flexilis* and *Pinus longaeva*. *For. Ecol. Manag.* **494**, 119277 (2021).
13. Jevon, F. V. et al. Experimental and observational evidence of negative conspecific density dependence in temperate ectomycorrhizal trees. *Ecology* **103**(11), e3808 (2022).
14. Wei, B. L. et al. Differences in density dependence among tree mycorrhizal types affect tree species diversity and relative growth rates. *Plants* **11**(18), 2340 (2022).

15. Twieg, B. D., Durall, D. M. & Simard, S. W. Ectomycorrhizal fungal succession in mixed temperate forests. *New Phytol.* **176**(2), 437–447 (2007).
16. Boeraeve, M., Honnay, O. & Jacquemyn, H. Effects of host species, environmental filtering and forest age on community assembly of ectomycorrhizal fungi in fragmented forests. *Fungal Ecol.* **36**, 89–98 (2018).
17. Lutz, J. A. et al. Global importance of large-diameter trees. *Glob. Ecol. Biogeogr.* **27**(7), 849–864 (2018).
18. Beiler, K. J., Simard, S. W. & Durall, D. M. Topology of tree–mycorrhizal fungus interaction networks in xeric and mesic Douglas-fir forests. *J. Ecol.* **103**(3), 616–628 (2015).
19. Guo, M. S. et al. Community composition of ectomycorrhizal fungi associated with *Pinus sylvestris* var. *mongolica* plantations of various ages in the Horqin Sandy Land. *Ecol. Ind.* **110**, 105860 (2020).
20. Henkel, T. W. & Mayor, J. R. Implications of a long-term mast seeding cycle for climatic entrainment, seedling establishment, and persistent monodominance in a Neotropical, ectomycorrhizal canopy tree. *Ecol. Res.* **34**(4), 472–484 (2019).
21. Delevich, C. A., Koch, R. A., Aime, M. C. & Henkel, T. W. Ectomycorrhizal fungal community assembly on seedlings of a Neotropical monodominant tree. *Biotropica* **53**(6), 1486–1497 (2021).
22. Rudawska, M. & Leski, T. Ectomycorrhizal fungal assemblages of nursery-grown Scots pine are influenced by age of the seedlings. *Forests* **12**(2), 134 (2021).
23. Zhang, J. et al. Fine-scale species co-occurrence patterns in an old-growth temperate forest. *For. Ecol. Manag.* **257**(10), 2115–2120 (2009).
24. Hao, Z. Q. et al. Natural secondary poplar-birch forest in Changbai Mountain: species composition and community structure. *Chin. J. Plant. Ecol.* **32**(2), 251 (2008).
25. Nérée, O. & Kuyper, T. Importance of the ectomycorrhizal network for seedling survival and ectomycorrhiza formation in rain forests of south Cameroon. *Mycorrhiza* **12**(1), 13–17 (2002).
26. García de Jalón, L. et al. Microhabitat and ectomycorrhizal effects on the establishment, growth and survival of *Quercus ilex* L. seedlings under drought. *Plos One* **15**(6), e0229807 (2020).
27. Hou, J., Mi, X., Liu, C. & Ma, K. Spatial patterns and associations in a *Quercus-Betula* forest in northern China. *J. Veg. Sci.* **15**(3), 407–414 (2004).
28. Phillips, R. P., Brzostek, E. & Midgley, M. G. The mycorrhizal-associated nutrient economy: a new framework for predicting carbon–nutrient couplings in temperate forests. *New Phytol.* **199**(1), 41–51 (2013).
29. Kuang, J. et al. Root-associated fungal community reflects host spatial co-occurrence patterns in a subtropical forest. *ISME Commun.* **1**(1), 65 (2021).
30. Selosse, M., Richard, F. & Simard, S. Mycorrhizal networks: des liaisons dangereuses? *Trends Ecol. Evol.* **21**(11), 621–628 (2006).
31. Richard, F., Millot, S., Gardes, M. & Selosse, M. A. Diversity and specificity of ectomycorrhizal fungi retrieved from an old-growth Mediterranean forest dominated by *Quercus ilex*. *New Phytol.* **166**(3), 1011–1023 (2005).
32. Pec, G. J., Simard, S. W., Cahill, J. F. Jr & Karst, J. The effects of ectomycorrhizal fungal networks on seedling establishment are contingent on species and severity of overstorey mortality. *Mycorrhiza* **30**(2–3), 173–183 (2020).
33. Kennedy, P. G., Mielke, L. A. & Nguyen, N. H. Ecological responses to forest age, habitat, and host vary by mycorrhizal type in boreal peatlands. *Mycorrhiza* **28**(3), 315–328 (2018).
34. Põlme, S. et al. Host preference and network properties in biotrophic plant–fungal associations. *New Phytol.* **217**(3), 1230–1239 (2018).
35. Bono, L. M., Gensel, C. L., Pfennig, D. W. & Burch, C. L. Evolutionary rescue and the coexistence of generalist and specialist competitors: an experimental test. *Proc. Royal Soc. B: Biol. Sci.* **282**(1821), 20151932 (2015).
36. Sun, W. et al. Ectomycorrhizal fungi enhance the tolerance of phytotoxicity and cadmium accumulation in oak (*Quercus acutissima* Carruth.) seedlings: modulation of growth properties and the antioxidant defense responses. *Environ. Sci. Pollut. Res.* **29**(5), 6526–6537 (2022).
37. Zhang, R., Shi, X. F., Liu, P. G., Wilson, A. W. & Mueller, G. M. Host shift speciation of the ectomycorrhizal genus *Suillus* (Suillineae, Boletales) and biogeographic comparison with its host Pinaceae. *Front. Microbiol.* **13**, 831450 (2022).
38. Ouvrard, D., Chalise, P. & Percy, D. M. Host-plant leaps versus host-plant shuffle: a global survey reveals contrasting patterns in an oligophagous insect group (Hemiptera, Psylloidea). *Syst. Biodivers.* **13**(5), 434–454 (2015).
39. Lofgren, L., Nguyen, N. H. & Kennedy, P. G. Ectomycorrhizal host specificity in a changing world: can legacy effects explain anomalous current associations? *New Phytol.* **220**(4), 1273–1284 (2018).
40. Smith, J. E., Molina, R., Huso, M. M. P. & Larsen, M. J. Occurrence of *Piloderma fallax* in young, rotation-age, and old-growth stands of Douglas-fir (*Pseudotsuga menziesii*) in the Cascade Range of Oregon, USA. *Can. J. Bot.* **78**(8), 995–1001 (2000).
41. Lilleskov, E., Hobbie, E. A. & Horton, T. Conservation of ectomycorrhizal fungi: exploring the linkages between functional and taxonomic responses to anthropogenic N deposition. *Fungal Ecol.* **4**(2), 174–183 (2011).
42. Gilson, A. et al. Seasonal changes in carbon and nitrogen compound concentrations in a *Quercus petraea* chronosequence. *Tree Physiol.* **34**(7), 716–729 (2014).
43. Hutchison, L. J. & Piché, Y. J. Effects of exogenous glucose on mycorrhizal colonization in vitro by early-stage and late-stage ectomycorrhizal fungi. *Can. J. Bot.* **73**(6), 898–904 (1995).
44. Petersen, P. M. The ecology of Danish soil inhabiting Pezizales with emphasis on edaphic conditions. *Nord. J. Bot.* **5**(1), 98 (1985).
45. Song, Z., Liu, Y., Su, H. & Hou, J. N-P utilization of *Acer mono* leaves at different life history stages across altitudinal gradients. *Ecol. Evol.* **10**(2), 851–862 (2019).
46. Hobbie, E. A. & Agerer, R. Nitrogen isotopes in ectomycorrhizal sporocarps correspond to belowground exploration types. *Plant. Soil.* **327**, 71–83 (2010).
47. Kyaschenko, J., Clemmensen, K. E., Hagenbo, A., Karltun, E. & Lindahl, B. D. Shift in fungal communities and associated enzyme activities along an age gradient of managed *Pinus sylvestris* stands. *ISME J.* **11**(4), 863–874 (2017).
48. Põlme, S. et al. Fungaltraits: a user-friendly traits database of fungi and fungus-like stramenopiles. *Fungal Divers.* **105**(1), 1–16 (2020).
49. Bai, Z. et al. Ectomycorrhizal fungus-associated determinants jointly reflect ecological processes in a temperature broad-leaved mixed forest. *Sci. Total Environ.* **703**, 135475 (2020).
50. Yang, H. Distribution patterns of dominant tree species on northern slope of Changbai Mountain. *Res. Ecosyst.* **5**, 1–14 (1985).
51. Yan, T. et al. Ectomycorrhizal fungi respiration quantification and drivers in three differently-aged larch plantations. *Agric. For. Meteorol.* **265**, 245–251 (2019).
52. Romano, N., Lignola, G., Brigante, M., Bosso, L. & Chirico, G. Residual life and degradation assessment of wood elements used in soil bioengineering structures for slope protection. *Ecol. Eng.* **90**, 498–509 (2016).
53. Smith, M. G., Miller, R. E., Arndt, S. K., Kasel, S. & Bennett, L. T. Whole-tree distribution and temporal variation of non-structural carbohydrates in broadleaf evergreen trees. *Tree Physiol.* **38**(4), 570–581 (2018).
54. Tedersoo, L. et al. Shotgun metagenomes and multiple primer pair-barcode combinations of amplicons reveal biases in metabarcoding analyses of fungi. *MycoKeys* **10**, 1–43 (2015).
55. Bolyen, E. et al. Reproducible, interactive, scalable and extensible microbiome data science using Qiime 2. *Nat. Biotechnol.* **37**(8), 852–857 (2019).
56. Callahan, B. J. et al. Dada2: High-resolution sample inference from Illumina amplicon data. *Nat. Methods*. **13**(7), 581–583 (2016).
57. Kõljalg, U. et al. Towards a unified paradigm for sequence-based identification of fungi. *Mol. Ecol.* **22**(21), 5271–5277 (2013).

58. Chong, J., Liu, P., Zhou, G. & Xia, J. Using MicrobiomeAnalyst for comprehensive statistical, functional, and meta-analysis of microbiome data. *Nat. Protoc.* **15**(3), 799–821 (2020).
59. Foster, Z. S., Sharpton, T. J., Grünwald, N. J. & Metacoder: an R package for visualization and manipulation of community taxonomic diversity data. *PLoS Comput. Biol.* **13**(2), e1005404 (2017).
60. Oksanen, J. et al. Vegan: community ecology package. R package version 2.5-7 (2020).
61. Kothe, E. et al. The ectomycorrhizal community of urban linden trees in Gdańsk, Poland. *Plos One* **16**(4), e0237551 (2021).
62. Csardi, G. & Nepusz, T. The igraph software package for complex network research. *InterJournal Complex. Syst.* **1695** (2006).
63. Zhang, B. G., Zhang, J., Liu, Y., Shi, P. & Wei, G. H. Co-occurrence patterns of soybean rhizosphere microbiome at a continental scale. *Soil Biol. Biochem.* **118**, 178–186 (2018).
64. Yang, Y. et al. Elevation-related climate trends dominate fungal co-occurrence network structure and the abundance of keystone taxa on Mt. Norikura, Japan. *Sci. Total Environ.* **799**, 149368 (2021).
65. Ma, B. et al. Geographic patterns of co-occurrence network topological features for soil microbiota at continental scale in eastern China. *ISME J.* **10**(8), 1891–1901 (2016).
66. Jiao, S. et al. Core microbiota in agricultural soils and their potential associations with nutrient cycling. *Msystems* **4**(2), e00313–00318 (2019).
67. Berry, D. & Widder, S. Deciphering microbial interactions and detecting keystone species with co-occurrence networks. *Front. Microbiol.* **5**, 219 (2014).
68. Bastian, M., Heymann, S. & Jacomy, M. Gephi: an open source software for exploring and manipulating networks. *Int. AAAI Conf. Weblogs Social Media*. **3**(1), 361–362 (2009).
69. Segata, N. et al. Metagenomic biomarker discovery and explanation. *Genome Biol.* **12**, 1–18 (2011).
70. Blankenberg, D. et al. Galaxy: a web-based genome analysis tool for experimentalists. *Curr. Protoc. Mol. Biol.* **19**, 1–21 (2010).

Acknowledgements

This research was financed by the National Natural Science Foundation of China (Project Nos. U2102220, 32371732, 32270017), and the Fund of CAS Key Laboratory of Forest Ecology and Silviculture, Institute of Applied Ecology, CAS (No. KLFES-2028).

Author contributions

DXZ and HSY designed the research. YWY and SAL performed the experiments. DXZ and ZB conducted the data analysis. DXZ and ZB wrote the original manuscript draft. DXZ and YWY performed the field sampling work. YLW and HSY acquired the funding. All the authors contributed to the article and approved the submitted version.

Declarations

Competing interests

The authors declare no competing interests.

Additional information

Supplementary Information The online version contains supplementary material available at https://doi.org/10.1038/s41598-025-91411-3.

Correspondence and requests for materials should be addressed to H.-S.Y.